

RESEARCH ARTICLE

RasGAP mediates neuronal survival in *Drosophila* through direct regulation of Rab5-dependent endocytosis

Behzad Rowshanravan¹, Simon A. Woodcock^{1,*}, José A. Botella², Claudia Kiermayer³, Stephan Schneuwly² and David A. Hughes^{1,‡}

ABSTRACT

The GTPase Ras can either promote or inhibit cell survival. Inactivating mutations in Drosophila RasGAP (encoded by vap), a Ras GTPase-activating protein, lead to age-related brain degeneration. Genetic interactions implicate the epidermal growth factor receptor (EGFR)-Ras pathway in promoting neurodegeneration but the mechanism is not known. Here, we show that the Src homology 2 (SH2) domains of RasGAP are essential for its neuroprotective function. By using affinity purification and mass spectrometry, we identify a complex containing RasGAP together with Sprint, which is a Ras effector and putative activator of the endocytic GTPase Rab5. Formation of the RasGAP-Sprint complex requires the SH2 domains of RasGAP and tyrosine phosphorylation of Sprint. RasGAP and Sprint colocalize with Rab5-positive early endosomes but not with Rab7-positive late endosomes. We demonstrate a key role for this interaction in neurodegeneration: mutation of Sprint (or Rab5) suppresses neuronal cell death caused by the loss of RasGAP. These results indicate that the long-term survival of adult neurons in Drosophila is crucially dependent on the activities of two GTPases, Ras and Rab5, regulated by the interplay of RasGAP and Sprint.

KEY WORDS: Tyrosine phosphorylation, Sprint, Guanine-nucleotide-exchange factor, Rab5, *Drosophila*, RasGAP, Vap

INTRODUCTION

Growth factors that signal through receptor tyrosine kinases (RTKs), such as the neurotrophins, have long been known to promote the survival of vertebrate neurons (Levi-Montalcini and Angeletti, 1963). Withdrawal of these growth factors or blocking of their signal transduction pathways leads to cell death (Raff et al., 1993). Two major signaling pathways involved in RTK-mediated neuronal survival are the mitogen-activated protein kinase (MAPK) and phosphoinositide 3-kinase (PI3K) signaling pathways (Reichardt, 2006). Both of these pathways are regulated by the small GTPase Ras, which is activated downstream of RTKs. The ability of Ras to promote neuronal survival is evolutionarily conserved: in *Drosophila*, Ras prevents apoptosis

¹The Faculty of Life Sciences, University of Manchester, Oxford Road, Manchester M13 9PT, UK. ²Lehrstuhl für Entwicklungsbiologie, Universität Regensburg, 93040 Regensburg, Germany. ³Research Unit Comparative Medicine, Helmholtz Zentrum München, German Research Center for Environmental Health (GmbH), Ingolstaedter Landstrasse 1, 85764 Neuherberg, *Present address: Discovery Sciences, AstraZeneca, Alderley Park, Cheshire SK10 4TG, UK.

[‡]Author for correspondence (david.a.hughes@manchester.ac.uk)

in the eye by inhibiting expression of the pro-apoptotic gene *hid* (Bergmann et al., 1998; Kurada and White, 1998).

Although Ras signaling can promote cell survival, there is evidence from experiments in cell culture that it can also promote cell senescence and cell death through autophagy (Chi et al., 1999; Elgendy et al., 2011; Kitanaka and Kuchino, 1999; Serrano et al., 1997; Young et al., 2009). In mammals, evidence that Ras is detrimental to neuronal survival in vivo is limited, but gene knockouts of two negative regulators of Ras, p120-Ras GTPaseactivating protein (p120-RasGAP/RASA1) and brain-specific synaptic RasGAP (synGAP), cause extensive neuronal apoptosis (Henkemeyer et al., 1995; Knuesel et al., 2005). Further evidence that Ras can promote neuronal cell death in vivo comes from mutants of the Drosophila RasGAP gene (vap), the homolog of mammalian p120-RasGAP/RASA1. RasGAP mutant flies show age-related cell death in neurons, with the dying neurons showing morphological features of autophagy (Botella et al., 2003). Analysis of the RasGAP mutant flies indicated that excessive signaling through the EGFR-Ras pathway leads to neurodegeneration, indicating that RasGAP plays an important role in ensuring the appropriate strength of signaling for neuronal survival. From this previous study, however, it was not clear which Ras effector pathway(s) were responsible for mediating neurodegeneration or whether RasGAP might be acting independently of Ras by binding to other proteins through its Src homology 2 and 3 (SH2 and SH3)

In this study, we have sought to determine the functional role of RasGAP in the neuronal survival by combining biochemical and genetic approaches. We show that the SH2 domains of RasGAP are essential in promoting neuronal survival in the adult Drosophila brain. We identify a number of partners that interact with RasGAP in a manner that is dependent on its SH2 domains, one of which is Sprint, the *Drosophila* homolog of the mammalian Ras-interacting proteins RIN1-RIN3, which act as guanine-nucleotide-exchange factors (GEFs) for Rab5 and related small GTPases (Kajiho et al., 2003; Saito et al., 2002; Tall et al., 2001). We demonstrate colocalization of RasGAP and Sprint with Rab5-positive early endocytic vesicles and show that the neurodegeneration observed in the RasGAP (vap) mutant flies is mediated through Sprint. This indicates a role for the Sprint-RasGAP interaction in regulating Ras-dependent Rab5 endocytic activity and we propose that the regulation of Rab5 activity through RasGAP and Sprint is necessary for neuronal survival in the adult brain of Drosophila.

RESULTS

RasGAP SH2 domains are essential for its neuroprotective function

In order to determine the functions of the RasGAP SH2 and SH3 domains in the neurons of the adult *Drosophila* brain, we crossed

flies carrying the vap^2 hypomorphic allele to UAS-GFP control and various UAS-RasGAP constructs (Fig. 1A) expressed under the control of the pan-neuronal driver ELAV-GAL4 (Robinow and White, 1988). Expression of the wild-type RasGAP (RasGAP^{WT}) and SH3-inactivated RasGAP (RasGAP^{SH23*2}) constructs rescued the neurodegeneration phenotype of the vap mutant flies (Fig. 1C,D,F). However, the GFP control and RasGAP double-SH2-inactivated (RasGAP^{SH2*32*}) constructs failed to rescue the vap mutant phenotype (Fig. 1B,E,F). This indicates that the SH2 domains of RasGAP play an essential role in mediating neuronal survival in the adult brain of Drosophila.

Identification of RasGAP SH2 interacting partners

In order to identify RasGAP-SH2-interacting proteins, RasGAP was tagged at its C-terminus with the localization and affinity purification (LAP) tag, consisting of GFP and 6×His (supplementary material Fig. S2A), so that RasGAP protein complexes could be affinity purified after expression of the tagged protein in S2 cells. LAP-tagged RasGAPSH2*32* was also used in order to classify interacting proteins as either SH2phosphotyrosine dependent or independent. RasGAP-LAP proteins were expressed in S2 cells, purified from lysates with anti-GFP antibodies (GFP-Trap), and co-purifying tyrosine-phosphorylated proteins were detected by western blotting. Five distinct bands at ~220, 200, 130, 110 and 60 kDa were observed in the RasGAP^{WT} pulldown (supplementary material Fig. S2B). These bands were entirely absent in the RasGAPSH2*32* and GFP control pulldowns, indicating that these phosphotyrosine-containing proteins interact with RasGAP in an SH2-dependent manner. The 130-kDa phosphotyrosine protein band (supplementary material Fig. S2B, large arrowhead) corresponds to the tagged RasGAPWT molecular mass and it might represent tyrosine-phosphorylated RasGAP.

Larger scale purifications were separated by SDS-PAGE, and gel slices at molecular mass regions corresponding to the major tyrosine-phosphorylated interacting proteins were excised (supplementary material Fig. S2C) and processed for mass spectrometry (MS). The results (unweighted spectral counts, defined as the total number of fragmentation spectra that map to peptides of a given protein) from two independent but parallel

experiments were then quantified as mean normalized spectral counts and hierarchically clustered on the basis of uncentered Pearson's correlation (Fig. 2) showing relative amounts of each protein co-purifying with each of the three constructs. The complete cluster output is listed in supplementary material Table S1. Three main clusters of proteins were identified (Fig. 2A). Within the RasGAP clusters, there are several subclusters including 155 RasGAP SH2-independent binding partners (Fig. 2A1,A2) and 115 SH2-dependent binding partners of RasGAP (Fig. 2B).

RasGAP SH2 domains enrich for the YxxPxD consensus binding sequence

After analyzing the protein sequences of RasGAP-interacting proteins, using regular expression analysis, 14 RasGAP SH2dependent interacting proteins (underlined in Fig. 2B) were found to contain the YxxPxD RasGAP SH2-binding consensus sequence. This constitutes 12.2% of the identified proteins that show RasGAP SH2-dependent binding, which is a significantly higher percentage of YxxPxD-containing proteins than that found in RasGAP SH2-independent interacting proteins (7.1%) or the entire *Drosophila melanogaster* proteome (5.1%) (supplementary material Table S2). This indicates that RasGAP SH2 domains enrich for proteins containing the YxxPxD RasGAP SH2-binding consensus sequence. If only the most abundant interacting proteins are considered [proteins with higher than four (0.001) normalized) spectral counts], five out of 14 proteins contain YxxPxD (highlighted in bold in Fig. 2B), which equates to 35.7% YxxPxD enrichment. This suggests a correlation between the abundance of SH2-dependent interacting partners of RasGAP and YxxPxD enrichment.

RasGAP is tyrosine-phosphorylated in an SH2-dependent manner

MS analysis of proteins in the 130 kDa region showed that RasGAP^{WT} was phosphorylated on tyrosine 363 (pTyr363) residue [(K)AAEKIYATLR(E)] (supplementary material Table S3). The (K)AAEKIYTLR(E) peptide fragment was detected in two independent experiments but only a small fraction of peptide was tyrosine-phosphorylated (data not shown). This finding suggests that only a fraction of the overexpressed

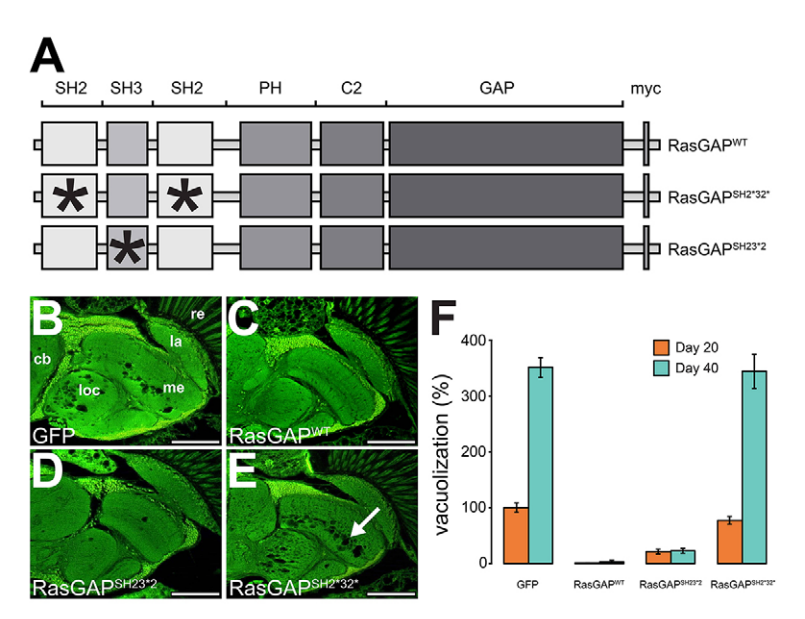


Fig. 1. RasGAP SH2 domains are essential for its neuroprotective function. (A) Schematic representation of the RasGAP-Myc fusion protein constructs used in this study. C2, Ca²⁺dependent phospholipid-binding domain; GAP, GTPase-activating protein; PH, pleckstrin homology domain; SH2/3, Src homology 2/3 domain. Head sections from vap2 flies expressing (B) UAS-GFP, (C) UAS-RasGAPWT-Myc, (D) UAS-RasGAPSH23*2-Myc, and (E) UAS-RasGAP^{SH2*32*}–Myc under the control of the pan-neuronal driver ELAV-GAL4. cb, central brain; la, lamina; loc, lobula complex; me, medulla; re, retina. Scale bars: 50 μm. (F) The percentage vacuolization of the stocks relative to the GFP control were assessed at 20 or 40 days. Data are represented as mean±s.e.m. Statistical significance was tested by one-way ANOVA and Dunnett's multiple comparison test. For day 20 and 40, all stocks compared to the GFP control were significantly different (P<0.001) except for the RasGAPSH2*32*. The arrow shows neurodegeneration (vacuolization).

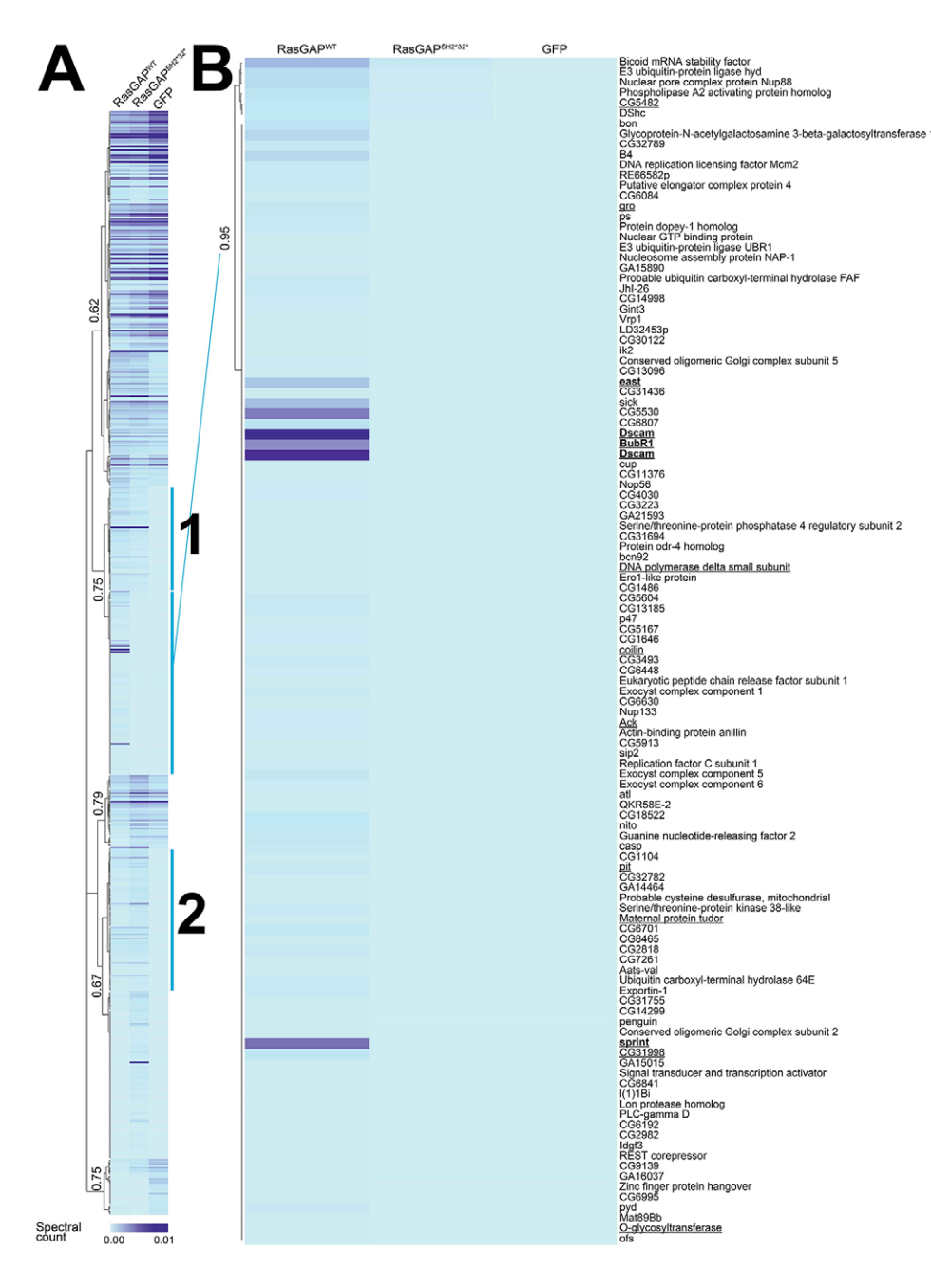


Fig. 2. Unsupervised hierarchical clustering of RasGAP-interacting proteins. (A) The figure displays the relative abundance (mean normalized spectral counts) of each protein between the different MS analyzed biological samples, which have been hierarchically clustered on the basis of uncentered Pearson's correlation and displayed at 6.33% saturation at 0.01 maximum spectral count. The protein hits are from Drosophila melanogaster (DROME) and Drosophila pseudoobscura (DROPS) species. The proteins with high relative abundance are indicated with dark blue and proteins with low relative abundance are indicated with light blue. There are three main clusters of proteins identified, including clusters of proteins enriched to all three (RasGAPWT, RasGAPSH2*32* and GFP) conditions (correlation 0.62 and 0.79), clusters of proteins enriched to RasGAP (correlation 0.75 and 0.67) and clusters of proteins enriched to GFP control (correlation 0.75). Within the RasGAP clusters, there are several subclusters including (A1 and A2) 155 RasGAP-binding partners where binding was independent of the RasGAP SH2 domains, and (B) 115 binding partners that were dependent on the RasGAP SH2 domains. The SH2-dependent interacting proteins containing the YxxPxD RasGAP SH2-binding consensus sequence are underlined and proteins with higher than 0.001 normalized spectral counts are

RasGAP is phosphorylated on tyrosine residue 363. Tyrosine phosphorylation of RasGAP^{SH2*32*} was not detected, indicating the importance of the RasGAP SH2 domains in mediating RasGAP tyrosine phosphorylation.

Association of RasGAP with Sprint requires the SH2 domains of RasGAP and tyrosine phosphorylation of Sprint

From the 115 proteins that showed RasGAP SH2-dependent interaction, Sprint had one of the largest relative abundance differences between the RasGAP and RasGAP and RasGAP samples. This potential interaction was particularly interesting as Sprint, like RasGAP, interacts with Ras (Jékely et al., 2005). As well as its Ras association domain at the C-terminus, Sprint has an SH2 domain and a vacuolar protein sorting 9 (VPS9)-like domain found in Rab5 GEFs (see Fig. 4A). We initially confirmed that wild-type RasGAP and Sprint form a complex (Fig. 3A), and determined the mechanism of Sprint–RasGAP association by

using GFP-tagged Sprint^{WT} to pulldown a number of RasGAP mutant constructs. RasGAP interacted with Sprint in an SH2-dependent manner given that Sprint failed to interact with full-length RasGAP^{SH2*32*} (Fig. 3A). Moreover, the isolated N-terminal SH2–SH3–SH2 region of RasGAP was sufficient to interact with Sprint, whereas inactivation of the SH3 domain had no effect on the interaction. RasGAP mutant constructs with either a catalytically inactive GAP domain (GAP*) or a conserved site of tyrosine phosphorylation mutated (Y363F) still interacted with Sprint. Taken together, these results show that the SH2 domains alone are necessary and sufficient for the Sprint–RasGAP interaction. Either of the two SH2 domains was sufficient to bind to Sprint (Fig. 3A).

highlighted in bold.

In order to determine whether Sprint interaction with RasGAP SH2 domains depends on Sprint tyrosine phosphorylation, GFP-tagged Sprint^{WT}-expressing S2 cells were lysed in the presence or absence of the inhibitor of tyrosine phosphatases, sodium

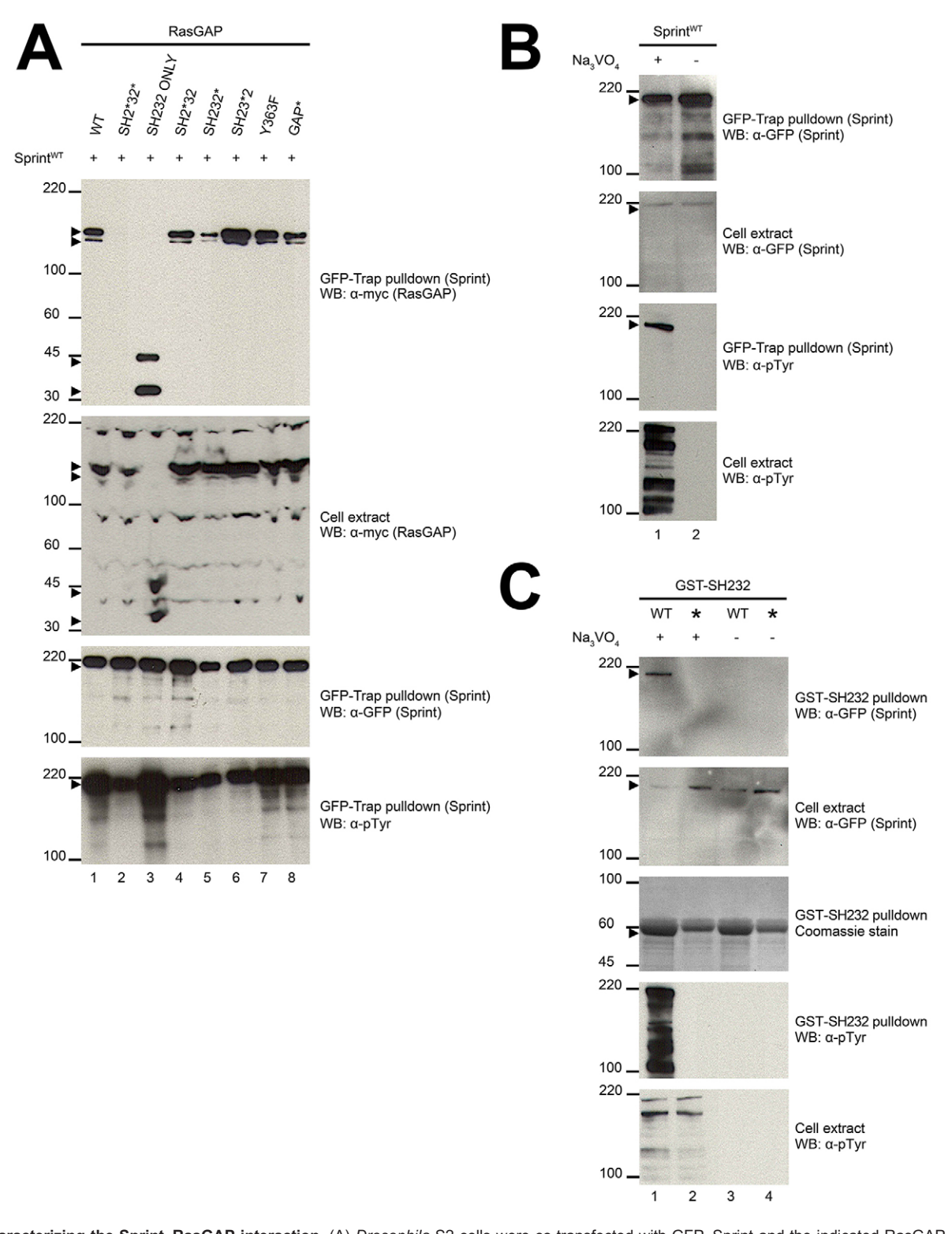


Fig. 3. Characterizing the Sprint–RasGAP interaction. (A) *Drosophila* S2 cells were co-transfected with GFP–Sprint and the indicated RasGAP–Myc constructs. GFP-Trap affinity beads were used to immunoprecipitate GFP–Sprint from S2 cell lysates. Immunoprecipitates and samples of the cell extracts were western blotted with anti-Myc antibodies to detect RasGAP–Myc, anti-GFP to detect GFP-Sprint and anti-phosphotyrosine (pTyr) to detect tyrosine-phosphorylated GFP–Sprint. (B) *Drosophila* S2 cells were transfected with GFP–Sprint and lysed in the presence or absence of sodium orthovanadate (Na₃VO₄). GFP-Trap was used to immunoprecipitate GFP–Sprint, and immunoprecipitates and cell extracts were western blotted with anti-GFP to detect GFP–Sprint, and anti-pTyr to detect tyrosine-phosphorylated GFP–Sprint. (C) Wild-type (WT) and double-SH2-inactivated (*) GST–SH232 bound to Agarose 4B beads was used to pull down GFP–Sprint from the lysates analyzed in B. The pulldowns and cell extracts were western blotted with anti-GFP to detect GFP–Sprint, and anti-pTyr to detect tyrosine-phosphorylated GFP–Sprint. The GST–SH232 proteins were stained in an SDS-PAGE gel using Coomassie stain. Arrowheads indicate the relevant protein bands.

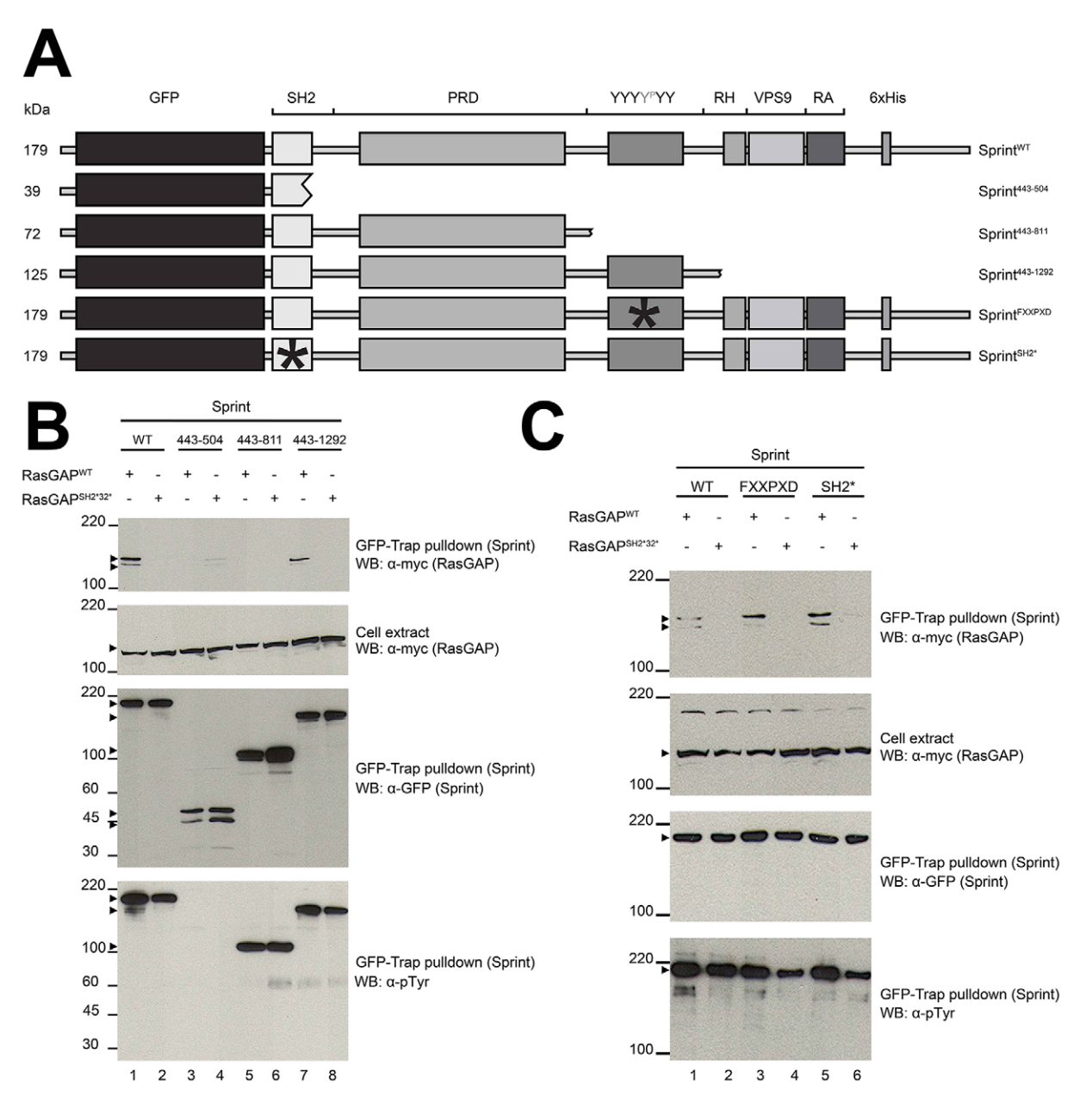


Fig. 4. Identifying the region of Sprint responsible for mediating the Sprint–RasGAP interaction. (A) Schematic representation of the GFP–Sprint fusion protein constructs used in this study. PRD, proline-rich domain; RA, Ras association domain; RH, RIN homology domain; Y^P, phosphotyrosine. (B,C) *Drosophila* S2 cells were co-transfected with GFP–Sprint and RasGAP–Myc constructs. The GFP-Trap affinity beads were used to pulldown Sprint from S2 cell lysate and the immunoprecipitates were western blotted using anti-pTyr, anti-GFP and anti-Myc antibodies. Arrowheads indicate the relevant protein bands. The apparent difference in Sprint^{FXXPXD} tyrosine phosphorylation when co-expressed with mutant RasGAP compared to RasGAP^{WT} is not seen consistently.

orthovanadate (Na₃VO₄), and GST-tagged RasGAP SH232^{WT} and SH2*32* domains were then used to pulldown GFP–Sprint^{WT}. Sprint was tyrosine-phosphorylated when lysates were prepared in the presence of Na₃VO₄ (Fig. 3B) and tyrosine-phosphorylated Sprint interacted with RasGAP SH2 domains (Fig. 3C). When lysates were prepared in the absence of Na₃VO₄, Sprint was not tyrosine-phosphorylated and did not interact with RasGAP SH2 domains. Sprint only associated with intact RasGAP SH2 domains because it failed to interact with GST–SH2*32*.

In order to narrow down the region of Sprint responsible for mediating phosphotyrosine-dependent Sprint-RasGAP association,

a number of Sprint-truncated constructs were used to pulldown RasGAP (Fig. 4A). RasGAP was found to interact with ΔVPS9 Sprint (Sprint 443–1292) but failed to interact with shorter Sprint 443–811 and Sprint 443–504 constructs (Fig. 4B), even though Sprint 443–811 was tyrosine phosphorylated (Fig. 4B). This suggests that the region from 812 to 1292, which encompasses six tyrosine residues, is responsible for mediating the Sprint–RasGAP interaction (Fig. 4B). One of those six tyrosine residues on Sprint (Y1056) was found to be phosphorylated (supplementary material Table S3) and corresponds to the YxxPxD RasGAP SH2-binding consensus sequence. To assess whether Y1056 is required for the RasGAP SH2 interaction with

Sprint, GFP-tagged Sprint was mutated at Y1056 (Fig. 4A). However, RasGAP efficiently associated with the Sprint YxxPxD mutant (Sprint^{FXXPXD}) (Fig. 4C). This indicates that Sprint Y1056 is not essential for association with RasGAP SH2. The level of tyrosine phosphorylation of Sprint^{FXXPXD} was similar to Sprint^{WT}, with any differences reflective of inefficient western blot transfer, indicating that there are other phosphotyrosine residues within Sprint that contribute to the Sprint–RasGAP interaction (Fig. 4C). As expected, Sprint^{443–504}, which contains no tyrosine residues, failed to show any tyrosine phosphorylation (Fig. 4B) and did not interact with RasGAP.

Sprint has a single SH2 domain that could play a part in binding to tyrosine-phosphorylated RasGAP. However, a Sprint construct with an inactivated SH2 domain (Sprint^{SH2*}, Fig. 4A) did not affect the Sprint–RasGAP interaction (Fig. 4C). As mentioned above, mutation of the tyrosine phosphorylation site of RasGAP (Y363) also did not affect Sprint–RasGAP binding (Fig. 3A). These results show that neither the SH2 domain of Sprint nor tyrosine phosphorylation of RasGAP at Y363 is required for the Sprint–RasGAP interaction.

Sprint and RasGAP colocalize in cytoplasmic punctate structures

RasGAP and Sprint constructs were overexpressed in S2 cells and their cellular localization was determined by fluorescence microscopy. Sprint^{WT} and RasGAP^{WT} colocalized in punctate structures within the cytoplasm (Fig. 5A,B), and this

colocalization depended on the SH2 domains of both Sprint and RasGAP being intact (Fig. 5A,B) as constructs with inactivated SH2 domains showed a diffuse cytoplasmic distribution (Fig. 5A). When expressed separately, Sprint localized to multiple cytoplasmic puncta in an SH2-dependent manner whereas RasGAP had a diffuse cytoplasmic distribution (Fig. 5C,D). This indicates that the expression of Sprint leads to the translocation of RasGAP to cytoplasmic puncta.

Sprint and RasGAP colocalize with Rab5-positive early endocytic vesicles

In order to assess the nature of Sprint puncta, S2 cells expressing Sprint were treated with Dynasore, an inhibitor of the GTPase dynamin that has a key role in the early stages of endocytosis (Macia et al., 2006). Dynasore inhibited fluid phase uptake of Dextran in untransfected S2 cells indicating that it effectively blocked endocytosis under these experimental conditions (Fig. 6A,B). Dynasore treatment significantly reduced the number of Sprint puncta within 15 minutes (Fig. 6A–C). This strongly indicates that Sprint puncta are endocytic structures, whose formation depends on the GTPase activity of dynamin.

Sprint is a VPS9-containing protein and a putative GEF for Rab5 (Jékely et al., 2005). In order to assess whether Sprint is capable of associating and colocalizing with Rab5, S2 cells were co-transfected with Sprint and Rab5 constructs. Sprint interacted with Rab5 in a nucleotide-dependent manner, interacting strongly with wild-type and dominant-negative (DN) Rab5, but not with

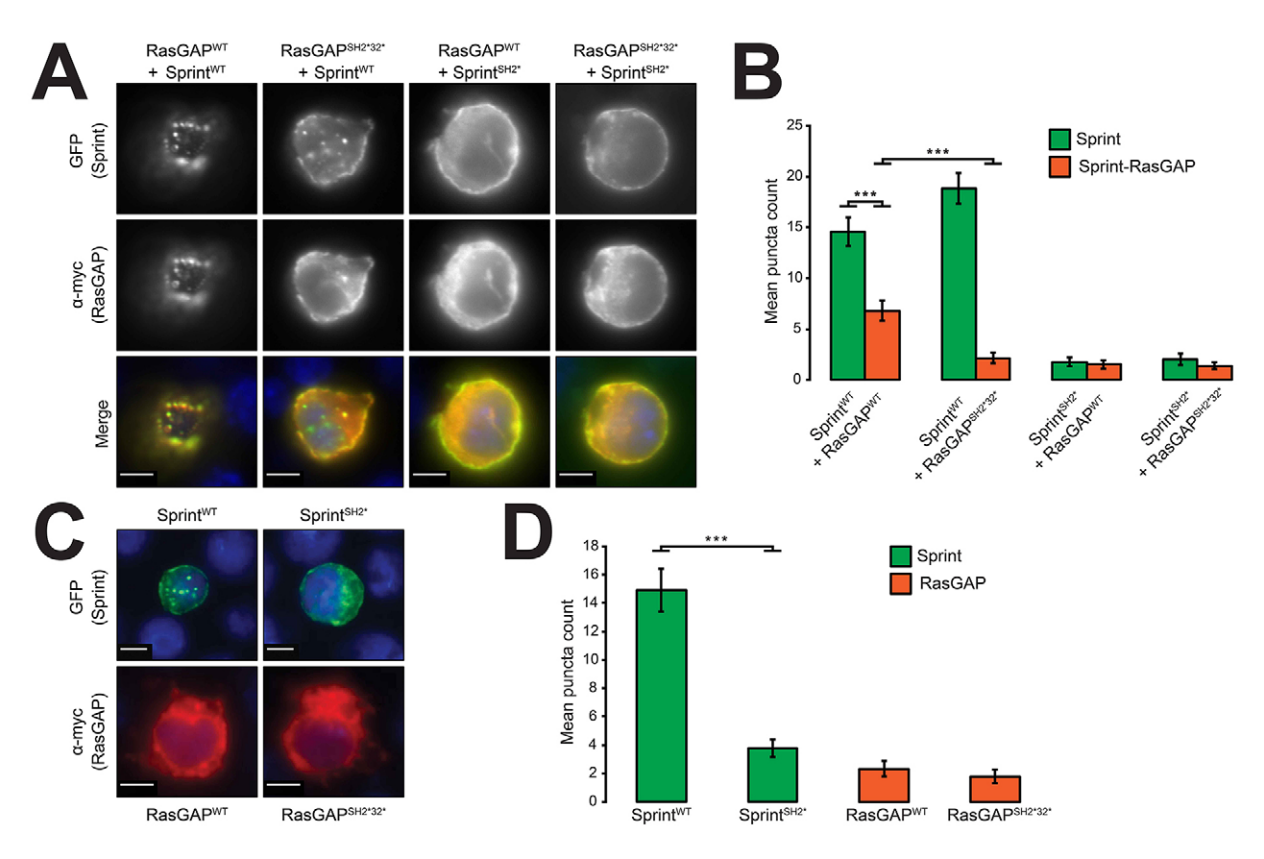


Fig. 5. Sprint and RasGAP colocalize in cytoplasmic punctate structures. (A) *Drosophila* S2 cells were co-transfected with Sprint and RasGAP constructs and the localization of each protein was visualized by immunohistochemistry and fluorescence microscopy. In the merged channel, Sprint is shown in green and RasGAP is shown in red. (B) The number of Sprint puncta per cell (green bars) and RasGAP puncta colocalizing with Sprint puncta (red bars) were recorded ($n \ge 34$). (C,D) The number of puncta per cell was determined for cells expressing either Sprint^{WT}, Sprint^{SH2*}, RasGAP^{WT} or RasGAP^{SH2*32*} constructs ($n \ge 42$). Data are represented as mean \pm s.e.m. Statistical significance was tested by one-way ANOVA and *** indicates a significant difference between sample means (P < 0.001). Scale bars: 5 μm.

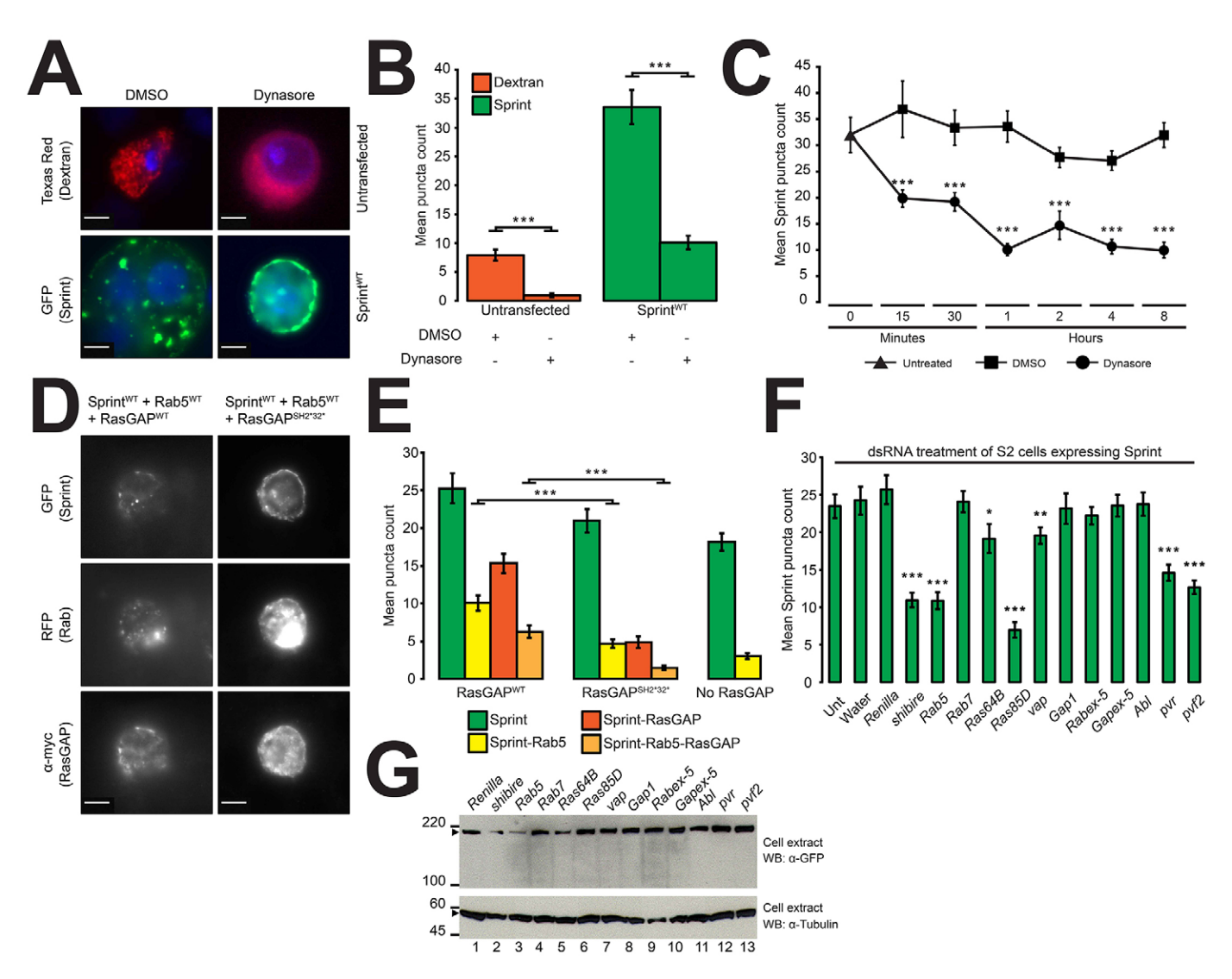


Fig. 6. Sprint and RasGAP colocalize with Rab5-positive early endocytic vesicles. (A) Drosophila GFP-Sprint^{WT}-transfected or untransfected (Dextran) S2 cells were treated with DMSO or Dynasore for 1 hour. (B) The number of Sprint (green bars) or Dextran (red bars) puncta per cell was recorded ($n \ge 30$). (C) The number of GFP-Sprint^{WT} puncta per cell was recorded ($n \ge 36$) in a time course. The cells were either untreated or treated with DMSO or Dynasore. (D) Drosophila S2 cells were co-transfected with Rab5, Sprint and RasGAP constructs and the localization of each protein was visualized by immunohistochemistry and fluorescence microscopy. (E) The number of Sprint puncta per cell (green bars), Rab5 (yellow bars) and RasGAP (red bars) puncta colocalizing with Sprint puncta, and Sprint puncta colocalizaing with both Rab5 and RasGAP (orange bars) were recorded ($n \ge 33$). (F,G) Drosophila S2 cells were transfected with GFP-Sprint^{WT} and were either left untreated (Unt), or treated with water or dsRNA, and the number of puncta per cell were recorded ($n \ge 37$) and compared against control (Renilla dsRNA). S2 cell lysates from dsRNA treated cells were western blotted using anti-GFP and anti-tubulin antibodies. Arrowheads indicate the relevant protein bands. Data are represented as mean±s.e.m. ***P<0.001; **P<0.01; *P<0.05 (one-way ANOVA). Scale bars: 5 μ m.

constitutively-active (CA) Rab5 (supplementary material Fig. S3A). Sprint failed to interact with wild-type Rab7 or Rab11 (supplementary material Fig. S3A). Sprint colocalized with Rab5 in a VPS9-dependent manner but failed to colocalize with Rab7 (supplementary material Fig. S3B,C). In order to assess whether Sprint and RasGAP colocalize with Rab5-positive early endocytic vesicles, Sprint, RasGAP and Rab5 constructs were co-expressed in S2 cells. Sprint and RasGAP colocalized with Rab5-positive early endocytic vesicles (Fig. 6D) and this colocalization was dependent on the RasGAP SH2 domains being intact (Fig. 6E).

In order to assess whether the number of Sprint puncta is dependent on RTK signaling or endocytosis, we performed RNA interference (RNAi) in S2 cells expressing GFP-tagged Sprint by treating them with double-stranded RNA (dsRNA) (Brown,

2010). The number of Sprint puncta was significantly reduced (*P*<0.001) compared to control (*Renilla* dsRNA) when S2 cells were treated with dsRNA against *shibire* (the *Drosophila* dynamin homolog), *Rab5*, *Ras85D* (Ras homolog), *Pvr* or *Pvf2* (a RTK and its ligand, respectively) (Fig. 6F). However, the number of Sprint puncta was not affected when S2 cells were treated with dsRNA targeting *Rab7* or two other putative Rab5 GEFs, *Rabex-5* (Yan et al., 2010) and *Gapex-5* (FlyBase annotation symbol CG1657). Treatment with most dsRNAs had no effect on the level of GFP–Sprint^{WT} expression except for some decrease with *shibire* and *Rab5* (Fig. 6G). These results suggest that the localization of Sprint to early endosomes is regulated not only by components involved in the early stages of endocytosis (dynamin and Rab5) but also by components

involved in RTK signaling, such as PVR, PVF2 and Ras. These results are consistent with a model where Sprint associates with endocytosed RTKs such as PVR (Fig. 8).

Mutant Sprint or Rab5 suppresses the *vap* mutant neurodegenerative phenotype in the adult *Drosophila* brain

In order to assess whether Sprint functions together with RasGAP in controlling neuronal survival in the adult brain, genetic interactions between RasGAP (vap) and Sprint mutations were investigated. The neurodegenerative phenotype of the vap² mutant was significantly suppressed (P<0.001) when spri was mutated homozygously (Fig. 7B,D,G); a weaker, but still significant, suppression was observed when flies were heterozygous for spri (Fig. 7H). As Sprint is proposed to activate Rab5, genetic interactions between RasGAP and Rab5 were also investigated. Heterozygosity for Rab5 hypomorphic $(Rab5^4/+)$ and null $(Rab5^2/+)$ alleles significantly suppressed the vap mutant neurodegeneration phenotype (Fig. 7B,F,G) with the Rab5-null allele showing the stronger suppression (Fig. 7G). The Sprint and Rab5 mutations alone had no discernible phenotype in the adult brain (Fig. 7C,E,G). These genetic interactions are consistent with a model where RasGAP, Sprint and Rab5 act within the same pathway to control neuronal survival.

DISCUSSION

Regulation of neuronal survival by RasGAP-Sprint-Rab5

The Ras oncoprotein has seemingly contradictory roles in regulating cell survival; in some cells Ras promotes cell survival, whereas in others it causes cell death by triggering apoptosis or autophagy. In the adult *Drosophila* brain overactivation of Ras, resulting from mutation of its negative regulator RasGAP, leads to age-related neurodegeneration. In this study, we present evidence that the age-related neurodegeneration caused by Ras overactivation is the result of dysregulation of Rab5, a crucial regulator of the early steps in endocytosis.

We identified a new association between RasGAP and Sprint, a putative GEF for Rab5 (Jékely et al., 2005). Formation of the RasGAP-Sprint complex required the SH2 domains of RasGAP and tyrosine phosphorylation of Sprint. Although these observations are consistent with direct binding of the RasGAP SH2 domains to phosphotyrosine residues on Sprint, we cannot exclude the possibility that the interaction is indirect, mediated by an adaptor protein(s). Sprint localized with Rab5-positive early endocytic vesicles, similar to the localization of its mammalian homologs RIN1-RIN3 (Kajiho et al., 2003; Kimura et al., 2006; Tall et al., 2001), and RasGAP colocalized with Sprint endocytic puncta. As both proteins interact with activated RTKs it is possible that the colocalization observed in S2 cells reflects their separate recruitment to endocytosed RTKs. However, a Sprint protein with an inactivated SH2 domain, which would be unable to bind to an RTK, still associated with RasGAP, indicating that the colocalization observed is likely to be the result of formation of a RasGAP-Sprint complex, independent of their separate association with RTKs.

Similar to its *Drosophila* homolog Sprint, mammalian RIN1 consists of VPS9-like, SH2 and Ras association domains (Fig. 4A), which can bind to Rab5, RTKs and Ras, respectively. RIN1 has been shown to mediate Ras-activated endocytosis through its activation of Rab5 (Tall et al., 2001) and to regulate receptor-mediated endocytosis (Hu et al., 2008). *Drosophila* S2 cells express the RTK PVR (Sims et al., 2009), and Sprint has been shown to bind directly to PVR using its SH2

domain (Jékely et al., 2005). Knockdown of PVR or its ligand PVF2 significantly reduced the number of Sprint endocytic puncta, consistent with at least some Sprint puncta being associated with endocytosed active PVR. Our identification of a RasGAP-Sprint complex suggests an attractive model to explain how the activation of Sprint by GTP-bound Ras might be regulated (Fig. 8). Tyrosine phosphorylation of Sprint, either by RTKs or by the cytoplasmic tyrosine kinase Abl (Hu et al., 2005), would recruit RasGAP to early endosomes and allow localized regulation of Ras-GTP levels and the GEF activity of Sprint. This in turn would modulate the rate of Rab5-mediated RTK endocytosis (Tall et al., 2001). The interaction and subsequent signaling of Sprint, Rab5 and Abl determines the fate of endocytosed receptors (Balaji et al., 2012). To directly test whether RasGAP regulates Rab5 activity in S2 cells, we developed a pulldown assay using GST-Rabenosyn-5 (Mottola et al., 2010) to quantify the levels of Rab5-GTP in cell extracts. We investigated whether Rab5-GTP levels changed when S2 cells overexpress RasGAP, Sprint or the PVR receptor tyrosine kinase, but did not see significant changes in overall Rab5-GTP levels. This analysis is complicated by the existence of other putative Rab5 GEFs (Yan et al., 2010) and perhaps different pools of Rab5 in cells, making it difficult to detect localized changes in Rab5-GTP levels. Because of the difficulty of measuring Rab5-GTP levels in vitro we investigated genetic interactions between mutations in the RasGAP (vap), Sprint and Rab5 genes in vivo.

The model we propose (Fig. 8) predicts that loss of RasGAP function (in a *vap* mutant) would cause increased endocytosis of RTKs through increased levels of local Ras-GTP resulting in activation of Sprint and overactivation of Rab5. In the Drosophila adult brain, genetic interactions indicate that the vap mutant neurodegenerative phenotype is the result of enhanced EGFR signaling (Botella et al., 2003), and there is evidence in other tissues in *Drosophila* that progression through the endocytic pathway can indeed enhance EGFR signaling (Chanut-Delalande et al., 2010; Miura et al., 2008). Our observations that mutation of Sprint or Rab5 suppresses the vap mutant neurodegeneration phenotype are consistent with dysregulation of Rab5 activity as the cause of the neurodegeneration and indicate a crucial role for RasGAP in restraining Rab5 activity in neurons. A concern with our genetic interaction studies is that the suppression observed could be caused by unrecognized second site mutations rather than by the spri and Rab5 mutations. Homozygous mutation of spri completely suppressed the vap mutant neurodegeneration phenotype, which is consistent with an essential role for Sprint in mediating the neuronal death resulting from loss of RasGAP, but, as only one allele of spri was tested, this result could be caused by an unrecognized second site mutation. Although both *Rab5* alleles were derived from the same P element (transposon) line and should have the same genetic background, we found a stronger suppression of the vap mutant neurodegenerative phenotype by the Rab5-null allele $(Rab5^2)$ compared to the Rab5 hypomorphic allele $(Rab5^4)$, showing that the level of neurodegeneration correlates with the level of Rab5 activity. Taking the *vap* genetic interactions with *spri* and *Rab5* together, the results strongly support the conclusion that the brain neurodegeneration in vap mutant flies is the result of excessive activation of Rab5 by Sprint, but do not exclude the less likely possibility that independent second site mutations on the *spri* and *Rab5* mutant chromosomes suppress the *vap* mutant.

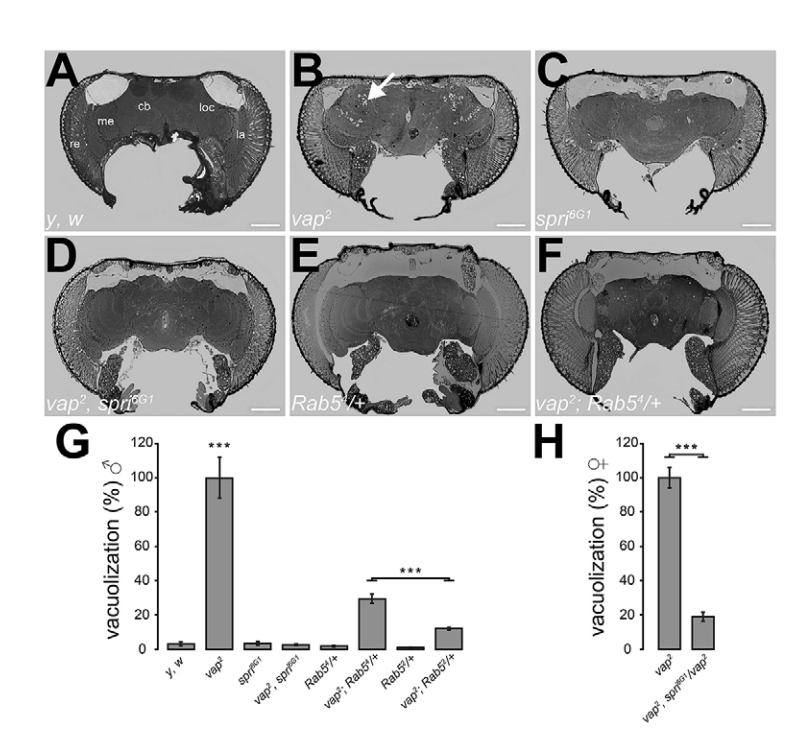


Fig. 7. Mutant Sprint or Rab5 suppresses the vap mutant neurodegenerative phenotype in the adult Drosophila brain. (A–F) Flies of the indicated genotypes were aged for 18–20 days, and their heads were sectioned and photographed. The arrow shows neurodegeneration (vacuolization). cb, central brain; la, lamina; loc, lobula complex; me, medulla; re, retina. Scale bars: 100 μ m. (G,H) The percentage vacuolization of the male (σ) and female (φ) stocks relative to vap^2 was assessed ($n \ge 3$). Data are represented as mean \pm s.e.m. ***P<0.001 (one-way ANOVA).

New proteins that interact with RasGAP SH2 domains

This study has shown that *Drosophila* proteins that interact with RasGAP in a SH2-dependent manner are enriched for the YxxPxD RasGAP-SH2-binding consensus sequence, which was originally deduced from mammalian phosphopeptide selection experiments (Songyang et al., 1993) and studies on known RasGAP interacting proteins such as p190-RhoGAP (Hu and Settleman, 1997). This demonstrates that RasGAP SH2 domains are likely to bind to phosphorylated YxxPxD sequences in order to mediate their interaction with other proteins, which is in agreement with the literature (Hu and Settleman, 1997; Woodcock and Hughes, 2004). However, given that most of the identified RasGAP SH2-dependent interacting partners did not have the YxxPxD RasGAP SH2-binding consensus sequence it

indicates either that there are a large number of false-positive partners that showed an SH2-dependent RasGAP interaction identified in this study, or that many of the interacting proteins do not bind directly to RasGAP, or that RasGAP SH2s can bind to phosphotyrosine residues different from YxxPxD. When a stringent spectral count cut-off was applied, the fraction of YxxPxD-containing partners increased threefold, indicating that binding partners co-purifying most efficiently with RasGAP are more likely to have the consensus binding sequence. Although this further supports phosphorylated YxxPxD as being a preferred SH2-binding site, even at this stringent cut-off the majority of binding partners (9/14, 64.3%) did not have the consensus sequence, suggesting that the SH2 domains can bind to nonconsensus phosphotyrosine residues.

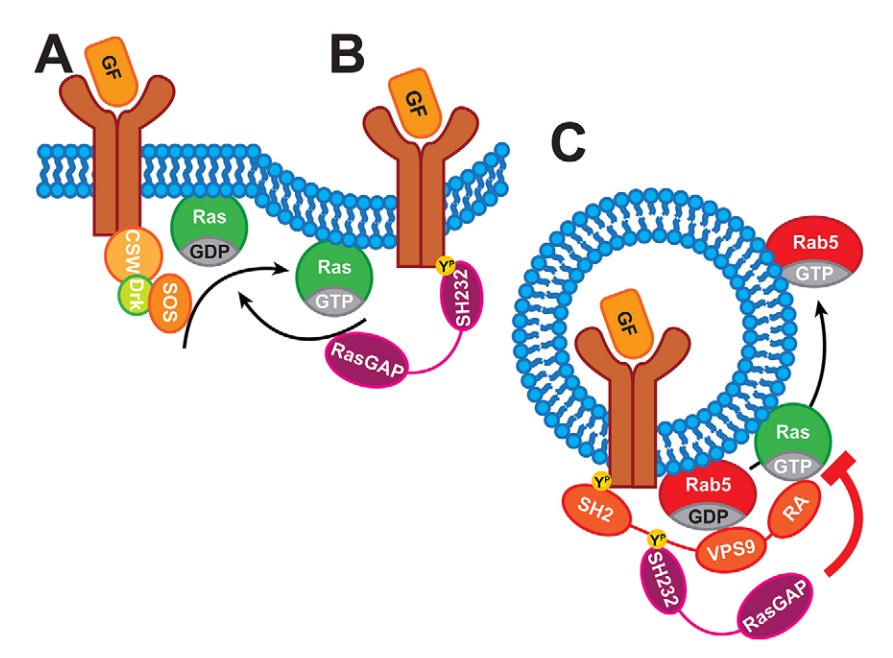


Fig. 8. RasGAP regulation of Rab5-dependent endocytosis. (A) Upon growth factor (GF) binding to RTKs, the SOS RasGEF is recruited to the receptor, in association with the adaptor proteins CSW and Drk, where it activates Ras. (B) RasGAP can associate with activated RTKs and deactivate Ras. (C) In early endosomes, Sprint associates with activated RTKs and its Rab5-GEF activity is stimulated by Ras-GTP. Tyrosine-phosphorylation of Sprint allows recruitment of RasGAP to early endosomes (shown here as direct binding to Sprint). RasGAP deactivates Ras on early endosomes and limits Sprintmediated Rab5 activation. RA, Ras association domain; YP, phosphotyrosine.

This study has identified several potential new partners for the SH2 RasGAP domains in Drosophila S2 cells. The RasGAP-SH2-interacting proteins with highest relative abundance in the pulldowns were Sprint (discussed above); Dscam, a cell adhesion molecule responsible for self-avoidance of sensory neuron dendrites (Matthews et al., 2007; Schmucker et al., 2000); BubR1, a kinetochore protein required for accurate chromosome segregation (Logarinho et al., 2004); and East, a nuclear protein responsible for the normal olfactory and gustatory responses of the adult Drosophila (VijayRaghavan et al., 1992; Wasser and Chia, 2000). None of these proteins have yet been identified as partners of mammalian p120-RasGAP. We have confirmed SH2dependent interaction with RasGAP for two of these proteins, tyrosine-phosphorylated Sprint (this study) and Dscam (Y. Long, B.R. and D.A.H., unpublished), but it will be important to validate the other potential interactions discovered. Based on this study (supplementary material Fig. S4), and previous findings, we have established that the interaction of RasGAP with RTKs, including EGFR and PVR, is evolutionarily conserved between flies and mammals but it is unclear whether non-RTK partners are also conserved. As this study is the first systematic investigation of the RasGAP SH2 interactome, it will be of great interest to determine whether the binding partners identified here are also partners of mammalian p120-RasGAP.

Conclusions

Our results suggest a new mechanism through which active Ras-GTP levels are regulated specifically on early endosomes by the association of RasGAP with Sprint, and that disruption of this pathway leads to neurodegeneration through dysregulation of Rab5 activity. The results are consistent with previous studies implicating Rab5 activity in neuronal survival: mutations in the mammalian Rab5-GEF amyotrophic lateral sclerosis 2 (ALS2) lead to motor neuron disease (Hadano et al., 2001; Otomo et al., 2003; Yang et al., 2001), and the Huntington's disease protein Huntingtin is a part of a Rab5 effector complex (Pal et al., 2006). Taken together, these findings show that neurons are particularly susceptible to disruption of Rab5-regulated endocytic pathways, which in *Drosophila* are regulated by a new RasGAP–Sprintmediated mechanism.

MATERIALS AND METHODS Construction of plasmids

and pUAST-RasGAPSH2*32*-LAP pUAST-RasGAP^{WT}-LAP constructs were produced by NheI-XbaI double digestion of pUAST-RasGAP^{WT}-myc and pUAST-RasGAP^{SH2*32*}-myc (Feldmann et al., 1999), respectively, allowing subcloning of the LAP construct from pIC111 (Cheeseman and Desai, 2005) as a NheI-XbaI fragment in the place of the Myc tag on pUAST-RasGAP backbone. The pUAST-RasGAP-myc and GST-tagged SH232 SH2-inactivated constructs carried amino acid replacements of highly conserved arginine residues to leucine residues (R110L and R278L), as described previously (Feldmann et al., 1999; Woodcock and Hughes, 2004). The pUAST-RasGAPSH23*2-myc, pUAST-RasGAP^{R695K}-myc and pUAST-RasGAP^{Y363F}-myc constructs carried W219A, R659K and Y363F mutations, respectively (Woodcock and Hughes, 2004). The pUAST and pGEX-KG-GST SH232 constructs are composed of RasGAP residues 83-343. The pUAST-GFP-SprintWT construct was produced by KpnI-XbaI sequential digest of pUASp-GFP-Sprint^{WT} construct (Jékely et al., 2005) allowing subcloning of GFP–Sprint^{WT} into the pUAST backbone empty vector as a *KpnI-XbaI* fragment (Brand and Perrimon, 1993). In order to make the pUAST-GFP-Sprint^{SH2*} construct, a highly conserved R485 was replaced with leucine using QuikChange lightening site-directed mutagenesis kit (Stratagene). In order to make the pUAST-GFP-Sprint^{FXXPXD} construct, Y1056 was replaced with a phenylalanine residue. In order to make the pUAST-GFP-Sprint^{VPS9DA/PA} construct D1599 and P1603 were replaced with alanine residues. The pUAST-GFP-Sprint^{443–504}, pUAST-GFP-Sprint^{443–811} and pUAST-GFP-Sprint^{443–1292} constructs were produced as *SanDI-XbaI*, *MreI-XbaI* and *PasI-XbaI* fragments, respectively. The amino acid residues are based on the sequence of Sprint-b (UniProt accession number Q8MQW8-2). The pUASp-YFP Rab5, Rab7 and Rab11 constructs have been described previously (Zhang et al., 2007). The pMT-RFP-Rab5^{WT} and pMT-RFP-Rab5^{WT} constructs were produced by *AgeI-XbaI* sequential digest of pm-RFP-Rab5^{WT} and pm-RFP-Rab7^{WT}, respectively, allowing subcloning of the constructs into the pMT/V5-His B backbone empty vector (Invitrogen) as *XbaI-EcoRV* fragments. The pUAST-attBlox-PVR^{WT}-GFP and pUAST-attBlox-EGFR^{WT}-GFP plasmids were kindly provided by Pernille Rorth (Inaki et al., 2012).

S2 cell maintenance, transfection and lysis

The semi-adherent Drosophila embryonic Schneider 2 (S2) cell line (Schneider, 1972) was maintained in Schneider's medium with Lglutamine and sodium bicarbonate (Invitrogen, Gibco), which was supplemented with added 10% foetal bovine serum (FBS) (Sigma and Invitrogen, Gibco) and 1% penicillin-streptomycin mixtures (Invitrogen, Gibco). Cells were seeded at 1.1×10^5 cells cm⁻² and after 24 hours incubation at 25 °C and atmospheric CO₂ they were transiently transfected with Effectene (QIAGEN) at $\sim 2.0 \times 10^5$ cells cm⁻² or 75% confluence. All pUAST- and pUASp-based plasmids were co-transfected with pMT-GAL4 to allow copper-inducible expression (Klueg et al., 2002). The transfected cells were induced 24 hours later using CuSO₄ at 1 mM and were lysed 48 hours later using either complete S2 cell lysis buffer [20 mM Tris-HCl pH 7.5, 2 mM EDTA, 150 mM NaCl, 10% glycerol, 1% Triton X-100, 5 mM NaF, 1 mM PMSF, 1 mM DTT, 5 mM Na₃VO₄ and 1×EDTA-free protease cocktail inhibitor (Roche)] or minimal S2 cell lysis buffer [20 mM Tris-HCl pH 7.5, 100 mM NaCl, 10% (v/v) glycerol, 1% (v/v) Triton X-100, 1 mM PMSF, 1 mM DTT, 1×EDTAfree protease cocktail inhibitor and with or without 5 mM Na₃VO₄] to assess the phosphotyrosine-dependent nature of protein interactions. The crude cell lysate was spun at 13,000 g at 4°C for 10 minutes to clear the lysate from debris, before being snap frozen in liquid nitrogen for storage

GST fusion protein expression and purification from Escherichia coli

GST fusion proteins were expressed in *E. coli* BL21(DE3) by induction with 0.5 mM isopropyl-1-thio- β -D-galactopyranoside (Fisher Scientific) to induce protein expression for 2 hours. Bacterial cells from 200 ml of culture were collected by centrifugation, re-suspended in 10 ml STE (10 mM Tris-HCl pH 7.5, 150 mM NaCl and 1 mM EDTA) containing 1 mM PMSF, 5 mM DTT and 1.5% (v/v) N-lauroyl-sarcosine (Sigma), before being lysed by sonicator ultrasonic processor XL 2020 (Misonix). Triton X-100 was added at 1% (v/v) to the cell lysate, before being centrifuged at 10,000 g in order to remove the cell debris. The supernatants were incubated with Protino Glutathione–Agarose-4B beads (MACHEREY-NAGEL) for 1 hour at 4°C. The beads were washed three times in 10 ml STE buffer and stored in STE, 50% (v/v) glycerol and 5 mM DTT at $-20\,^{\circ}$ C.

GFP-Trap and GST-based protein complex pulldown and immunoblotting

The cleared cell lysate was incubated with GFP-Trap agarose (Chromotek) or GST beads for 2 hours at 4°C before being washed three to five times with complete or minimal S2 cell lysis buffer. The beads were heated in sample buffer (Invitrogen) and reducing agent (Invitrogen) and the supernatant was loaded on 4–12% Bis-Tris SDS-PAGE gels (Invitrogen), allowing gel staining (SimplyBlue SafeStain, Invitrogen) and western blotting of the pulled down proteins. The samples were electroblotted and stained as previously described (Woodcock and Hughes, 2004) using either mouse monoclonal antiphosphotyrosine P-Tyr-100 (PY-100, Cell Signaling) antibody at 1:5000 dilution, mouse mixed monoclonal (clones 7.1 and 13.1) anti-GFP

(Boehringer Mannhem) antibody at 1:1000-1:3000 dilution or mouse monoclonal anti c-Myc 9E10 (AbD Serotec) antibody at 1:500-1:1000 dilution.

Protein mass spectrometry and data deposition

Bands of interest were dehydrated using acetonitrile followed by vacuum centrifugation. Dried gel pieces were reduced with 10 mM dithiothreitol and alkylated with 55 mM iodoacetamide. Gel pieces were then washed alternately with 25 mM ammonium bicarbonate followed by acetonitrile. This was repeated and the gel pieces were dried by vacuum centrifugation. Samples were digested with either trypsin (specificity: C-terminal to Asp/Glu), trypsin and Asp-N (specificity: N-terminal to Asp/Cys), trypsin and Glu-C (V8 specificity: C-terminal to Asp/Glu) or Elastase (specificity: none) overnight at 37°C. Digested samples were analyzed by LC-MS/MS using either (i) a NanoAcquity LC (Waters, Manchester, UK) coupled to a LTQ Velos (Thermo Fisher Scientific, Waltham, MA) mass spectrometer with peptides concentrated on a precolumn (20 mm×180 µm inner diameter, Waters), (ii) an UltiMate® 3000 Rapid Separation LC (RSLC, Dionex Corporation, Sunnyvale, CA) coupled to a LTQ Velos Pro (Thermo Fisher Scientific, Waltham, MA) mass spectrometer or (iii) an UltiMate® 3000 Rapid Separation LC (RSLC, Dionex Corporation, Sunnyvale, CA) coupled to an Orbitrap Elite (Thermo Fisher Scientific, Waltham, MA) mass spectrometer. For the LTQ Velos Pro and Orbitrap Elite samples were desalted first before peptide separation. The peptides were separated using a gradient from 92–99% of solution A (0.1% v/v formic acid in water) and 1–8% solution B (0.1% v/v formic acid in acetonitrile) to 25–33% solution B, in 45 min at 200–300 nl min $^{-1}$, using a 75-mm×250- μ m inner diameter 1.7 μ M BEH C18, analytical column (Waters). For the Orbitrap Elite and Velos, the mass tolerance for precursor ions were set at 5 ppm and 0.5 Da, respectively and the mass tolerance for fragment ions were set at 0.5 Da. Peak-lists were generated using Mascot Daemon 2.2 (Matrix Science UK) employing the extract_msn.exe utility and the data were searched using Mascot 2.2 (Matrix Science UK), against the Uniprot database with taxonomy of *Drosophila* (fruit flies) selected. Data were further validated and searched using Scaffold (Proteome Software, Portland, OR), which models the score distribution of the entire dataset of spectra (Humphries et al., 2009). With no MuDPIT analysis technique employed, Mascot generated search (.dat) files were queried against uniprot.v14_0 database, allowing pyro-carbamidomethylation of cysteine as a fixed modification and tyrosine, serine and threonine phosphorylation as well as methionine oxidation as a variable modification. The data were viewed using Scaffold, version 3.00.08, and the results were analyzed at 99% protein identification probability tolerance threshold, with minimum number of two peptides at 50% identification probability acceptance threshold for at least one spectra required for protein identification. The Scaffoldassigned false discovery rate (FDR) of the proteins within the dataset was 0.2%. Samples were validated for phospho-modifications using either Mascot Delta (MD)-score (Savitski et al., 2011) or manual inspection of the data when applicable.

The mass spectrometry proteomics data have been deposited to the ProteomeXchange Consortium (http://proteomecentral.proteomexchange. org) via the PRIDE partner repository (Vizcaíno et al., 2013) with the dataset identifier PXD000176 and doi of http://dx.doi.org/10.6019/PXD000176 (PRIDE accession numbers 28714–28755). The original Scaffold search output file is available on request.

Quantification using spectral counting and hierarchical clustering

The unweighted spectral counts assigned to each identified protein by Scaffold were used to calculate the relative abundance of each protein, across biological samples, using the Scaffold-assigned total number of identified spectra per biological sample (normalized spectral counts). This was done for each biological sample (RasGAPWT, RasGAPSH2*32* and GFP) and their two independent repeats and the results were expressed as an average for each protein (mean normalized spectral counts) (Humphries et al., 2009; Lundgren et al., 2010). The mean normalized spectral counts were hierarchically clustered using Gene

Cluster 3.0, version 1.50 (C Clustering Library), which hierarchically clustered protein hits on the basis of uncentered Pearson's correlation and calculated the distances between hits using a complete-linkage matrix. The gene cluster file outputs (.cdt and .gtr) were then visualized using Java TreeView, version 1.1.6r2.

Immunohistochemistry and imaging

The S2 cells were seeded on poly-L-lysine-coated (Sigma) glass coverslips placed in a six-well plate. The cells were subsequently fixed in 1 ml of 4% formaldehyde (Agar Scientific) for 30 minutes and washed twice with 1 ml of PBS before being incubated and permeabilized with PBS-T [1×MgCl₂ and CaCl₂ free PBS (Sigma) and 0.1% Triton X-100] for 15 minutes. Once blocked in PBS-BT [PBS-T and 0.5% BSA] overnight at 4°C, the cells were incubated with 50 µl of primary antibody for 2 hours at room temperature, diluted at 1:200 in PBS-BT. The cells were washed twice with PBS-T and incubated with 50 µl of goat antimouse Alexa Fluor 555 secondary antibody (Invitrogen) for 2 hours at room temperature diluted in PBS-BT at 1:200. Images were either collected on an Olympus BX51 upright microscope using a 100× 1.30 NA UPlan Fln objective and captured using a CoolSNAP HQ camera (Photometrics) through MetaVue software, version 7.1.0.0 (Molecular Devices), which collectively processed the images at 0.07 µm pixel⁻¹, or were collected on a Leica DM600B upright microscope using a 100× 1.40 NA HCX PL APO objective and captured using a Hamamatsu C10600-10B (ORCA-R2) digital camera through Leica MM AF Premier software, version 1.5.0 (Leica), which collectively processed the images at 0.09 µm pixel⁻¹. Specific band-pass filter sets for DAPI, FITC and Texas Red were used to prevent bleed through from one channel to the next. Images were then processed and analyzed blind to the genotype using MBF-ImageJ, version 1.47b. Fluorescent puncta were counted manually.

Endocytosis assay and RNAi knockdown

For the fluid-phase endocytosis assay, untransfected cells attached to poly-L-lysine-coated coverslips were incubated with 500 nM Dextran, Texas Red®, 3000 MW (Invitrogen) for 1 hour before being fixed and prepared for imaging. Transfected or untransfected S2 cells were treated with the dynamin GTPase inhibitor, Dynasore (Millipore) for the indicated times (at 100 µM in DMSO) before being fixed and prepared for imaging (Macia et al., 2006). For the RNAi knockdown experiments, the pUAST-GFP-Sprint WT transfected S2 cells were seeded in a six-well plate. The cells were serum starved 24 hours later in 4 ml of serum-free Schneider's medium for 1 hour, then 300 µl of the transfected cell suspension was added to the well of a 24-well plate that contained 2000 ng dsRNA (Brown, 2010) in 10 µl of ultrapure H₂O. The dsRNAs were incubated with the cells for 5–7 hours, allowing their uptake, before 300 µl of 20% FBS-supplemented Schneider's medium was added. The cells were then induced 24 hours later with 1 mM CuSO₄ for 48 hours to allow GFP-Sprint expression, and then processed for immunohistochemistry, imaging, lysis and western blotting.

Drosophila stocks and genetics

Flies were raised and crossed at 25°C according to standard procedures. The UAS-RasGAP-myc transgenic stocks have been described previously (Feldmann et al., 1999; Woodcock and Hughes, 2004), and the RasGAP-Myc proteins were expressed under control of an ELAV-GAL4 driver present on chromosome 3. Expression of the UAS-RasGAP constructs was confirmed by real-time reverse-transcriptase-polymerase chain reaction (PCR) analysis (LightCycler, Roche) (supplementary material Fig. S1A). The $spri^{6GI}$ mutant stock was obtained from Pernille Rorth (Jékely et al., 2005). The $Rab5^2$ and $Rab5^4$ mutant stocks (Wucherpfennig et al., 2003) were obtained from the Bloomington Stock Centre. The vap^2 and $spri^{6GI}$ alleles were recombined on the X chromosome to make the vap^2 , $spri^{6GI}$ double mutant stock; the genotype was confirmed by PCR analysis (supplementary material Fig. S1B).

Drosophila head sectioning and staining

For the genetic interaction experiments, male flies were aged for 18-20 days at $25\,^{\circ}$ C. The proboscis was removed and the heads were placed in

2% formaldehyde and 2% glutaraldehyde in 0.1 M HEPES buffer (pH 7.2) for 24 hours at 4°C. The tissue was washed three time with double-distilled water (ddH₂O) and post-fixed in reduced osmium [1% $OsO_4 + 1.5\% K_4Fe(CN)_6$ in 0.1 M sodium cacodylate buffer] for 1 hour. The tissue was washed three times with ddH2O and en bloc stained with 1% aqueous uranyl acetate for 1 hour before being washed three times again with ddH₂O and dehydrated once in 25%, 50%, 70%, 80% and 90% ethanol and three times in 100% ethanol for 10 minutes. The tissue was washed three times in propylene oxide before being placed in propylene oxide and low viscosity (LV) resin (TAAB Laboratories Equipment) medium mixes (75:25, 50:50 and 25:75) over 24-36 hours before being placed in 100% LV resin, which was changed three or four times over 24 hours. The tissue was then flat-embedded in LV resin and placed in the oven at 60°C for 24 hours before being horizontally sectioned with Reichert-Jung (Ultracut) microtome at a 2-µm thickness in a region of the head encompassing 80-180 µm thickness, starting from the base of the head near the proboscis. The sections were dried on to a microscope slide using a hotplate for 10-20 minutes before being stained with Toluidine Blue stain for 30 seconds and washed once with ddH₂O and dab dried with flat blue tissue paper. Images were collected on a Leica DM600B upright microscope using 10× 0.25 NA HI PLAN objective and captured using a Hamamatsu C10600-10B (ORCA-R2) digital camera through Leica MM AF Premier software, version 1.5.0 (Leica), which collectively processed the images at 0.92 µm pixel⁻¹. A visible-light band-pass filter set was used to image the samples. Images were analyzed using MBF-ImageJ, version 1.47b and processed using GIMP, version 2.8.4 (GIMP Development Team). The total area of central brain, lobula complex and medulla was measured and the percentage of the area showing vacuolization was calculated. Three heads and a minimum of three sections per head were used for each genotype. For the rescue experiments, Drosophila stocks were aged for either 20 or 40 days and the heads were sectioned, stained and phenotypically quantified as described previously (Botella et al., 2003). Fluorescence microscopy was used to image auto-fluorescence in the sections.

Acknowledgements

We thank Julian Selley, Stacey Warwood and David Knight from the Biological Mass Spectrometry Core Research Facility at the University of Manchester for the bioinformatics and mass spectrometric processing of the data; Peter March and Steven Marsden from the Bioimaging Core Facility at the University of Manchester for the bioimaging training, help and support provided; Samantha Forbes from the Faculty of Life Sciences EM Facility at the University of Manchester for processing, sectioning and staining fly heads; and Sanjai Patel from the Fly Facility at the University of Manchester for his help, support and training provided. The Bioimaging Facility microscopes used in this study were purchased with grants from BBSRC, the Wellcome Trust and the University of Manchester Strategic Fund, and the Fly Facility is supported by funds from the University of Manchester and the Wellcome Trust (grant number 087742/Z/08/Z). We thank the Sheffield RNAi Screening Facility, Biomedical Sciences, University of Sheffield, supported by the Wellcome Trust (grant number 084757) for providing RNAi libraries, laboratory space, bioinformatics tools and other support for the screen. We would like to thank Pernille Rorth and Iain Cheeseman for providing us with plasmids and fly stocks.

Competing interests

The authors declare no competing interests.

Author contributions

B.R. designed and performed the experiments, analyzed the data and wrote the paper. D.A.H. devised the project, designed the experiments and wrote the paper. J.A.B., C.K. and S.S. designed and performed the rescue experiments. S.A.W. produced the fly lines used in the rescue experiments and had an important input into the RNAi experiments.

Funding

We thank Jamshid Rowshanravan and Mohtaram Mashhadi (Mashhad, Iran) for supporting B.R. and for funding the project in Manchester.

Supplementary material

Supplementary material available online at http://jcs.biologists.org/lookup/suppl/doi:10.1242/jcs.139329/-/DC1

References

- Balaji, K., Mooser, C., Janson, C. M., Bliss, J. M., Hojjat, H. and Colicelli, J. (2012). RIN1 orchestrates the activation of RAB5 GTPases and ABL tyrosine kinases to determine the fate of EGFR. J. Cell Sci. 125, 5887-5896.
- Bergmann, A., Agapite, J., McCall, K. and Steller, H. (1998). The Drosophila gene hid is a direct molecular target of Ras-dependent survival signaling. *Cell* **95**, 331-341.
- Botella, J. A., Kretzschmar, D., Kiermayer, C., Feldmann, P., Hughes, D. A. and Schneuwly, S. (2003). Deregulation of the Egfr/Ras signaling pathway induces age-related brain degeneration in the Drosophila mutant vap. *Mol. Biol. Cell* 14, 241-250.
- Brand, A. H. and Perrimon, N. (1993). Targeted gene expression as a means of altering cell fates and generating dominant phenotypes. *Development* 118, 401-415.
- Brown, S. (2010). Institutional Profile: The Sheffield RNAi screening facility: a service for high-throughput, genome-wide Drosophila RNAi screens. Future Med. Chem 2, 1805-1812.
- Chanut-Delalande, H., Jung, A. C., Baer, M. M., Lin, L., Payre, F. and Affolter, M. (2010). The Hrs/Stam complex acts as a positive and negative regulator of RTK signaling during Drosophila development. *PLoS ONE* **5**, e10245.
- Cheeseman, I. M. and Desai, A. (2005). A combined approach for the localization and tandem affinity purification of protein complexes from metazoans. Sci. STKE 2005, pl1.
- Chi, S., Kitanaka, C., Noguchi, K., Mochizuki, T., Nagashima, Y., Shirouzu, M., Fujita, H., Yoshida, M., Chen, W., Asai, A. et al. (1999). Oncogenic Ras triggers cell suicide through the activation of a caspase-independent cell death program in human cancer cells. *Oncogene* 18, 2281-2290.
- Elgendy, M., Sheridan, C., Brumatti, G. and Martin, S. J. (2011). Oncogenic Ras-induced expression of Noxa and Beclin-1 promotes autophagic cell death and limits clonogenic survival. *Mol. Cell* 42, 23-35.
- Feldmann, P., Eicher, E. N., Leevers, S. J., Hafen, E. and Hughes, D. A. (1999). Control of growth and differentiation by Drosophila RasGAP, a homolog of p120 Ras-GTPase-activating protein. *Mol. Cell. Biol.* **19**, 1928-1937.
- Hadano, S., Hand, C. K., Osuga, H., Yanagisawa, Y., Otomo, A., Devon, R. S., Miyamoto, N., Showguchi-Miyata, J., Okada, Y., Singaraja, R. et al. (2001). A gene encoding a putative GTPase regulator is mutated in familial amyotrophic lateral sclerosis 2. Nat. Genet. 29, 166-173.
- Henkemeyer, M., Rossi, D. J., Holmyard, D. P., Puri, M. C., Mbamalu, G., Harpal, K., Shih, T. S., Jacks, T. and Pawson, T. (1995). Vascular system defects and neuronal apoptosis in mice lacking ras GTPase-activating protein. *Nature* 377, 695-701.
- Hu, K. Q. and Settleman, J. (1997). Tandem SH2 binding sites mediate the RasGAP-RhoGAP interaction: a conformational mechanism for SH3 domain regulation. EMBO J. 16, 473-483.
- Hu, H., Bliss, J. M., Wang, Y. and Colicelli, J. (2005). RIN1 is an ABL tyrosine kinase activator and a regulator of epithelial-cell adhesion and migration. Curr. Biol. 15, 815-823.
- Hu, H., Milstein, M., Bliss, J. M., Thai, M., Malhotra, G., Huynh, L. C. and Colicelli, J. (2008). Integration of transforming growth factor beta and RAS signaling silences a RAB5 guanine nucleotide exchange factor and enhances growth factor-directed cell migration. *Mol. Cell. Biol.* 28, 1573-1583.
- Humphries, J. D., Byron, A., Bass, M. D., Craig, S. E., Pinney, J. W., Knight, D. and Humphries, M. J. (2009). Proteomic analysis of integrin-associated complexes identifies RCC2 as a dual regulator of Rac1 and Arf6. Sci. Signal. 2, ra51.
- Inaki, M., Vishnu, S., Cliffe, A. and Rørth, P. (2012). Effective guidance of collective migration based on differences in cell states. *Proc. Natl. Acad. Sci.* USA 109, 2027-2032.
- Jékely, G., Sung, H. H., Luque, C. M. and Rørth, P. (2005). Regulators of endocytosis maintain localized receptor tyrosine kinase signaling in guided migration. Dev. Cell 9, 197-207.
- Kajiho, H., Saito, K., Tsujita, K., Kontani, K., Araki, Y., Kurosu, H. and Katada, T. (2003). RIN3: a novel Rab5 GEF interacting with amphiphysin II involved in the early endocytic pathway. *J. Cell Sci.* 116, 4159-4168.
- Kimura, T., Sakisaka, T., Baba, T., Yamada, T. and Takai, Y. (2006). Involvement of the Ras-Ras-activated Rab5 guanine nucleotide exchange factor RIN2-Rab5 pathway in the hepatocyte growth factor-induced endocytosis of E-cadherin. J. Biol. Chem. 281, 10598-10609.
- Kitanaka, C. and Kuchino, Y. (1999). Caspase-independent programmed cell death with necrotic morphology. *Cell Death Differ.* **6**, 508-515.
- Klueg, K. M., Alvarado, D., Muskavitch, M. A. and Duffy, J. B. (2002). Creation of a GAL4/UAS-coupled inducible gene expression system for use in Drosophila cultured cell lines. *Genesis* 34, 119-122.
- Knuesel, I., Elliott, A., Chen, H. J., Mansuy, I. M. and Kennedy, M. B. (2005). A role for synGAP in regulating neuronal apoptosis. Eur. J. Neurosci. 21, 611-621.
- Kurada, P. and White, K. (1998). Ras promotes cell survival in Drosophila by downregulating hid expression. Cell 95, 319-329.
 Lavi Mortalskiii, P. and Ameletti, P. L. (1963). Escaptial rale of the page growth.
- Levi-Montalcini, R. and Angeletti, P. U. (1963). Essential role of the nerve growth factor in the survival and maintenance of dissociated sensory and sympathetic embryonic nerve cells in vitro. Dev. Biol. 7, 653-659.
- Logarinho, E., Bousbaa, H., Dias, J. M., Lopes, C., Amorim, I., Antunes-Martins, A. and Sunkel, C. E. (2004). Different spindle checkpoint proteins monitor microtubule attachment and tension at kinetochores in Drosophila cells. *J. Cell Sci.* 117, 1757-1771.
- Lundgren, D. H., Hwang, S. I., Wu, L. and Han, D. K. (2010). Role of spectral counting in quantitative proteomics. Expert Rev. Proteomics 7, 39-53.

- Macia, E., Ehrlich, M., Massol, R., Boucrot, E., Brunner, C. and Kirchhausen, T. (2006). Dynasore, a cell-permeable inhibitor of dynamin. *Dev. Cell* 10, 839-850.
- Matthews, B. J., Kim, M. E., Flanagan, J. J., Hattori, D., Clemens, J. C., Zipursky, S. L. and Grueber, W. B. (2007). Dendrite self-avoidance is controlled by Dscam. Cell 129, 593-604.
- Miura, G. I., Roignant, J. Y., Wassef, M. and Treisman, J. E. (2008). Myopic acts in the endocytic pathway to enhance signaling by the Drosophila EGF receptor. *Development* 135, 1913-1922.
- Mottola, G., Classen, A. K., González-Gaitán, M., Eaton, S. and Zerial, M. (2010). A novel function for the Rab5 effector Rabenosyn-5 in planar cell polarity. *Development* 137, 2353-2364.
- Otomo, A., Hadano, S., Okada, T., Mizumura, H., Kunita, R., Nishijima, H., Showguchi-Miyata, J., Yanagisawa, Y., Kohiki, E., Suga, E. et al. (2003). ALS2, a novel guanine nucleotide exchange factor for the small GTPase Rab5, is implicated in endosomal dynamics. *Hum. Mol. Genet.* 12, 1671-1687
- Pal, A., Severin, F., Lommer, B., Shevchenko, A. and Zerial, M. (2006). Huntingtin-HAP40 complex is a novel Rab5 effector that regulates early endosome motility and is up-regulated in Huntington's disease. J. Cell Biol. 172. 605-618.
- Raff, M. C., Barres, B. A., Burne, J. F., Coles, H. S., Ishizaki, Y. and Jacobson, M. D. (1993). Programmed cell death and the control of cell survival: lessons from the nervous system. Science 262, 695-700.
- Reichardt, L. F. (2006). Neurotrophin-regulated signalling pathways. *Philos. Trans. R. Soc. B* **361**, 1545-1564.
- Robinow, S. and White, K. (1988). The locus elav of Drosophila melanogaster is expressed in neurons at all developmental stages. *Dev. Biol.* 126, 294-303
- Saito, K., Murai, J., Kajiho, H., Kontani, K., Kurosu, H. and Katada, T. (2002). A novel binding protein composed of homophilic tetramer exhibits unique properties for the small GTPase Rab5. J. Biol. Chem. 277, 3412-3418.
- Savitski, M. M., Lemeer, S., Boesche, M., Lang, M., Mathieson, T., Bantscheff, M. and Kuster, B. (2011). Confident phosphorylation site localization using the Mascot Delta Score. Mol. Cell Proteomics 10, M110 003830.
- Schmucker, D., Clemens, J. C., Shu, H., Worby, C. A., Xiao, J., Muda, M., Dixon, J. E. and Zipursky, S. L. (2000). Drosophila Dscam is an axon guidance receptor exhibiting extraordinary molecular diversity. *Cell* 101, 671-684.
- Schneider, I. (1972). Cell lines derived from late embryonic stages of Drosophila melanogaster. J. Embryol. Exp. Morphol. 27, 353-365.

- Serrano, M., Lin, A. W., McCurrach, M. E., Beach, D. and Lowe, S. W. (1997).

 Oncogenic ras provokes premature cell senescence associated with accumulation of p53 and p16INK4a. *Cell* 88, 593-602.
- Sims, D., Duchek, P. and Baum, B. (2009). PDGF/VEGF signaling controls cell size in Drosophila. *Genome Biol.* 10, R20.
- Songyang, Z., Shoelson, S. E., Chaudhuri, M., Gish, G., Pawson, T., Haser, W. G., King, F., Roberts, T., Ratnofsky, S., Lechleider, R. J. et al. (1993). SH2 domains recognize specific phosphopeptide sequences. *Cell* 72, 767-778.
- Tall, G. G., Barbieri, M. A., Stahl, P. D. and Horazdovsky, B. F. (2001). Rasactivated endocytosis is mediated by the Rab5 guanine nucleotide exchange activity of RIN1. Dev. Cell 1, 73-82.
- VijayRaghavan, K., Kaur, J., Paranjape, J. and Rodrigues, V. (1992). The east gene of Drosophila melanogaster is expressed in the developing embryonic nervous system and is required for normal olfactory and gustatory responses of the adult. Dev. Biol. 154, 23-36.
- Vizcaíno, J. A., Côté, R. G., Csordas, A., Dianes, J. A., Fabregat, A., Foster, J. M., Griss, J., Alpi, E., Birim, M., Contell, J. et al. (2013). The PRoteomics IDEntifications (PRIDE) database and associated tools: status in 2013. *Nucleic Acids Res.* 41, D1063-D1069.
- Wasser, M. and Chia, W. (2000). The EAST protein of drosophila controls an expandable nuclear endoskeleton. *Nat. Cell Biol.* **2**, 268-275.
- Woodcock, S. A. and Hughes, D. A. (2004). p120 Ras GTPase-activating protein associates with fibroblast growth factor receptors in Drosophila. *Biochem. J.* **380**, 767-774.
- Wucherpfennig, T., Wilsch-Bräuninger, M. and González-Gaitán, M. (2003). Role of Drosophila Rab5 during endosomal trafficking at the synapse and evoked neurotransmitter release. *J. Cell Biol.* **161**, 609-624.
- Yan, H., Jahanshahi, M., Horvath, E. A., Liu, H. Y. and Pfleger, C. M. (2010). Rabex-5 ubiquitin ligase activity restricts Ras signaling to establish pathway homeostasis in Drosophila. Curr. Biol. 20, 1378-1382.
- Yang, Y., Hentati, A., Deng, H. X., Dabbagh, O., Sasaki, T., Hirano, M., Hung, W. Y., Ouahchi, K., Yan, J., Azim, A. C. et al. (2001). The gene encoding alsin, a protein with three guanine-nucleotide exchange factor domains, is mutated in a form of recessive amyotrophic lateral sclerosis. *Nat. Genet.* 29, 160-165.
- Young, A. R., Narita, M., Ferreira, M., Kirschner, K., Sadaie, M., Darot, J. F., Tavaré, S., Arakawa, S., Shimizu, S., Watt, F. M. et al. (2009). Autophagy mediates the mitotic senescence transition. *Genes Dev.* 23, 798-803.
- Zhang, J., Schulze, K. L., Hiesinger, P. R., Suyama, K., Wang, S., Fish, M., Acar, M., Hoskins, R. A., Bellen, H. J. and Scott, M. P. (2007). Thirty-one flavors of Drosophila rab proteins. *Genetics* 176, 1307-1322.